CORA Cork Open Research Archive
Cartlann Taighde Oscailte Chorcaí

| | |
|---|---|
| Title | Magnetic field structure of the extended 3C 380 jet |
| Authors | Gabuzda, Denise;Cantwell, T. M.;Cawthorne, T. V. |
| Publication date | 2014 |
| Original Citation | Gabuzda, D. C., Cantwell, T. M. and Cawthorne, T. V. (2014) 'Magnetic field structure of the extended 3C 380 jet', Monthly Notices of the Royal Astronomical Society: Letters, 438(1), pp. L1-L5. doi: 10.1093/mnrasl/slt129 |
| Type of publication | Article (peer-reviewed) |
| Link to publisher's version | https://academic.oup.com/mnrasl/article-lookup/doi/10.1093/mnrasl/slt129 - 10.1093/mnrasl/slt129 |
| Rights | © 2013, the Authors. Published by Oxford University Press on behalf of the Royal Astronomical Society |
| Download date | 2026-11-05 18:38:44 |
| Item downloaded from | https://hdl.handle.net/10468/4956 |



UCC
University College Cork, Ireland
Coláiste na hOllscoile Corcaigh

Monthly Notices
of the
ROYAL ASTRONOMICAL SOCIETY

MNRASL **438,** L1–L5 (2014)
Advance Access publication 2013 November 18

doi:10.1093/mnrasl/slt129

# Magnetic field structure of the extended 3C 380 jet

D. C. Gabuzda,[1⋆] T. M. Cantwell[1] and T. V. Cawthorne[2]

[1] *Physics Department, University College Cork, Cork, Ireland*
[2] *Jeremiah Horrocks Institute, University of Central Lancashire, Preston PR1 2HE, UK*

Accepted 2013 September 12. Received 2013 September 9; in original form 2013 July 9

**ABSTRACT**

An earlier study of the complex jet of 3C 380 by Papageorgiou et al. revealed total intensity and polarization structure associated with a bright knot K1 about 0.7 arcsec from the core that was reminiscent of that expected for a conical shock wave. In this new study, 1.42, 1.66 and 4.99 GHz total intensity, polarization and Faraday rotation images are presented and analysed. These images were derived from observations with the Very Long Baseline Array plus one antenna of the Very Large Array, obtained in 2006 March. These new images confirm the overall magnetic field structure of the knot K1 indicated in the earlier observations. In addition, a clear Faraday rotation gradient has been detected across the jet, extending roughly from 10 to 30 mas (70–200 pc) along the jet from the core (a radial distance of approximately two beamwidths). The gradient spans roughly 3.5 beamwidths in the transverse direction, and the difference in the rotation measures on either side of the jet is 4–5$\sigma$, demonstrating that the detection of the gradient is firm. We interpret this transverse Faraday rotation gradient as reflecting systematic variation of the line-of-sight component of a helical or toroidal magnetic field ($B$) associated with the jet of 3C 380. These results provide evidence that the helical field arising due to the joint action of the rotation of the central black hole and its accretion disc and the jet outflow can survive to distances of hundreds of parsecs from the central engine.

**Key words:** magnetic fields – polarization – galaxies: active – galaxies: jets.

## 1 INTRODUCTION

The radio emission associated with active galactic nuclei (AGNs) is synchrotron emission, which can be linearly polarized up to about 75 per cent in optically thin regions, where the polarization angle $\chi$ is orthogonal to the projection of the magnetic field $B$ on to the plane of the sky, and up to 10–15 per cent in optically thick regions, where $\chi$ is parallel to the projected magnetic field $B$ (Pacholczyk 1970). Linear polarization measurements thus provide direct information about both the degree of order and the direction of the magnetic field giving rise to the observed synchrotron radiation.

Multifrequency very long baseline interferometry (VLBI) polarization observations also provide information about the parsec-scale distribution of the spectral index (optical depth) of the emitting regions, as well as Faraday rotation occurring between the source and observer. Faraday rotation of the plane of linear polarization occurs during the passage of the associated electromagnetic wave through a region with free electrons and a magnetic field with a non-zero component along the line of sight. When the Faraday rotation occurs outside the emitting region in regions of non-relativistic plasma, the amount of rotation is given by

$$\chi_{\rm obs} - \chi_o = \frac{e^3\lambda^2}{8\pi^2\epsilon_o m^2 c^3}\int n_{\rm e}\boldsymbol{B}\cdot{\rm d}\boldsymbol{l} \equiv {\rm RM}\lambda^2, \quad (1)$$

where $\chi_{\rm obs}$ and $\chi_o$ are the observed and intrinsic polarization angles, respectively, $-e$ and $m$ are the charge and mass of the particles giving rise to the Faraday rotation, usually taken to be electrons, $c$ is the speed of light, $n_{\rm e}$ is the density of the Faraday-rotating electrons, $\boldsymbol{B}\cdot{\rm d}\boldsymbol{l}$ is an element of the line-of-sight magnetic field, $\lambda$ is the observing wavelength and RM (the coefficient of $\lambda^2$) is the rotation measure (e.g. Burn 1966). Simultaneous multifrequency observations thus allow the determination of both the RM, which carries information about the electron density and magnetic field in the region of Faraday rotation, and $\chi_o$, which carries information about the intrinsic magnetic field geometry associated with the source.

Systematic gradients in the Faraday rotation have been reported across the parsec-scale jets of several AGN, interpreted as reflecting the systematic change in the line-of-sight component of a toroidal or helical jet magnetic field across the jet (most recent reports include Asada et al. 2010; Croke, O'Sullivan & Gabuzda 2010; Hovatta et al. 2012; Mahmud et al. 2013). Such fields would come about in a natural way as a result of the 'winding up' of an initial 'seed' field by the rotation of the central accreting objects (e.g. Nakamura, Uchida & Hirose 2001; Lovelace et al. 2002).

⋆ E-mail: d.gabuzda@ucc.ie

© 2013 The Authors
Published by Oxford University Press on behalf of the Royal Astronomical Society

The quasar 3C 380 has been extensively studied with VLBI, for example, by Polatidis & Wilkinson (1998) and Papageorgiou et al. (2006, henceforth P2006). On kiloparsec scales, 3C 380 has a one-sided jet with two bright knots, detected in both the radio and optical bands, embedded in a diffuse halo (Wilkinson et al. 1991; O'Dea et al. 1999), with two bright knots, K1 and K2, approximately 0.7 and 1.0 arcsec from the core (Kameno et al. 2000). The jet of 3C 380 is also one-sided on parsec scales, with a sharp apparent bend, roughly 9 mas from the core, at the position of a bright knot ('component A' of Polatidis & Wilkinson 1998). Various superluminal components have been monitored over 10–20 yr (Polatidis & Wilkinson 1998; Lister et al. 2009). Curiously, component A has been found to move superluminally along position angle $\sim -30^\circ$, somewhat offset from the direction back towards the core (i.e. this component is not moving strictly radially).

The 1.6 GHz space VLBI and 5 GHz Very Long Baseline Array (VLBA) polarization-sensitive observations of P2006 yielded a two-frequency RM map indicating relatively modest variations in the Faraday rotation in the region of the 3C 380 VLBI jet; these measurements were tentative, since the difference between the two polarization angles was subject to an ambiguity of $n\pi$. The high-sensitivity 1.6 GHz VLBA+phased Very Large Array (VLA) data of P2006 also revealed polarization associated with the knot K1 located about 0.7 arcsec from the VLBI core, which was reminiscent of that expected for a conical shock wave.

The new 1.42+1.66+4.99 GHz VLBI observations presented here were obtained to further investigate the total intensity and polarization structure of the knot K1, and to provide further information about the parsec- and decaparsec-scale RM distribution in the vicinity of 3C 380.

## 2 OBSERVATIONS AND REDUCTION

The 1.416+1.658+4.986 GHz observations analysed here were obtained on 2006 March 26 with the VLBA and one antenna of the VLA, at an aggregate data rate of 128 Mb $s^{-1}$ in dual-polarization mode. The total duration of the VLBI observations was about 5.5 h. The preliminary phase and amplitude calibration, polarization (D-term) calibration, electric vector position angle (EVPA) calibration and imaging were all carried out in the National Radio Astronomy Observatory (NRAO) AIPS package using standard techniques.

The compact polarized BL Lac object 1823+568 was used for the D-term calibration at all three frequencies. This was carried out using the AIPS task LPCAL, solving simultaneously for the source polarizations in a small number of individual VLBI components corresponding to groups of CLEAN components, identified by hand.

1823+568 also served as the EVPA calibrator at all three frequencies, due to its relatively simple and stable jet polarization structure. The EVPAs were calibrated using VLBA polarization observations of 1823+568 made at 1.358, 1.430, 1.493 and 1.665 GHz on 2010 July 29. Note that the jet polarization structures of radio BL Lac objects on decaparsec scales have been shown to be constant on time-scales of at least 4–5 yr (Hallahan & Gabuzda 2008; Healy & Gabuzda 2013), making it possible to use these observations for the EVPA calibration despite the significant time offset from the 2006 observations. First, a region of compact polarization in the jet that was clearly detected at all three of our frequencies, as well as in the 2010 observations, was identified. The fully calibrated observed EVPA ($\chi$) values for 2010 July 29 at 1.358, 1.430, 1.493 and 1.665 GHz were then plotted versus $\lambda^2$; this confirmed that the $\chi$ values displayed the linear dependence characteristic of Faraday rotation. Further, this $\lambda^2$ dependence was interpolated or extrapolated to the three frequencies at which the 2006 observations were made, yielding calibrated $\chi$ values at these three frequencies, properly taking into account the Faraday rotation to which each was subject in the observations. These were then compared to the observed $\chi$ values to calibrate the latter. The resulting 4.986 GHz polarization map of 1823+568 was in very good consistency with previously published maps of this AGN at 5 GHz and other centimetre wavelengths (Gabuzda et al. 1994; Lister & Homan 2005), and the 1.416 and 1.658 GHz polarization maps of 1823+568 were fully consistent with the maps for 2010 July. The required EVPA corrections (rotations in $\chi$) are $+47^\circ$ at 4.99 GHz, $-56^\circ$ at 1.66 GHz and $-30^\circ$ at 1.42 GHz. Due to the simple and stable polarization structure of the 1823+568 jet, this EVPA calibration should be subject to uncertainties no greater than $2^\circ$ at all three frequencies.

Due to the extended nature of the emission in 3C 380, the imaging of this source at the lower two frequencies was carried out initially using only the inner VLBA antennas and the VLA, before adding in the other antennas, similar to the procedure used by P2006. Maps of the distribution of the total intensity $I$ and Stokes parameters $Q$ and $U$ at each frequency were made, both with usual natural weighting, and with matched resolutions corresponding to the lowest frequency beam. The distributions of the polarized flux ($p = \sqrt{Q^2 + U^2}$) and polarization angle ($\chi = \frac{1}{2} \arctan \frac{U}{Q}$) were obtained from the $Q$ and $U$ maps using the AIPS task COMB. Maps of the RM were then constructed using the AIPS task RM, as well as in CASA, after first subtracting the effect of the integrated RM (presumed to arise in our Galaxy) from the observed polarization angles (the integrated RM value for 3C 380 was taken to be $+26$ rad $m^{-2}$; Rusk 1988), so that any residual Faraday rotation was due predominantly to thermal plasma in the vicinity of the AGN. The uncertainties in the RM were based on the uncertainties in $Q$ and $U$, which were, in turn, estimated using the approach of Hovatta et al. (2012). The output pixels in the RM maps were blanked when the RM uncertainty from the $\chi$ versus $\lambda^2$ fit exceeded specified values, indicated below in the text and figure captions.

## 3 RESULTS AND DISCUSSION

### 3.1 Observed polarization structure

Fig. 1 presents the 5 GHz total intensity image of 3C 380, which shows the inner jet, with superposed magnetic field vectors. The magnetic field vectors were obtained by rotating the observed polarization vectors, corrected for Galactic but not local Faraday rotation, by $90^\circ$. This image is in excellent agreement with the results of Cawthorne et al. (1993), Taylor (1998), P2006 and the MOJAVE project (Lister & Homan 2005, http://www.physics.purdue.edu/astro/MOJAVE/), and shows predominantly longitudinal jet magnetic field on these scales, with an abrupt rotation in the inferred magnetic field direction at the position of knot A, near the bend in the jet 9–10 mas from the core. The 5 GHz total intensity map seems to show hints of limb brightening beyond about 30 mas from the core.

Fig. 2 (left) presents our 1.4 GHz total intensity image of 3C 380, showing the inner VLBI jet and knot K1, together with a more detailed view of the knot K1 at a distance of about 0.7 arcsec from the core. These images are quite consistent with the 1.6 GHz images presented by P2006. The top-right panel of Fig. 2 shows the 1.4 GHz polarization map for K1, and the bottom-right panel the 1.4–1.6 GHz RM map for this same region. The polarization

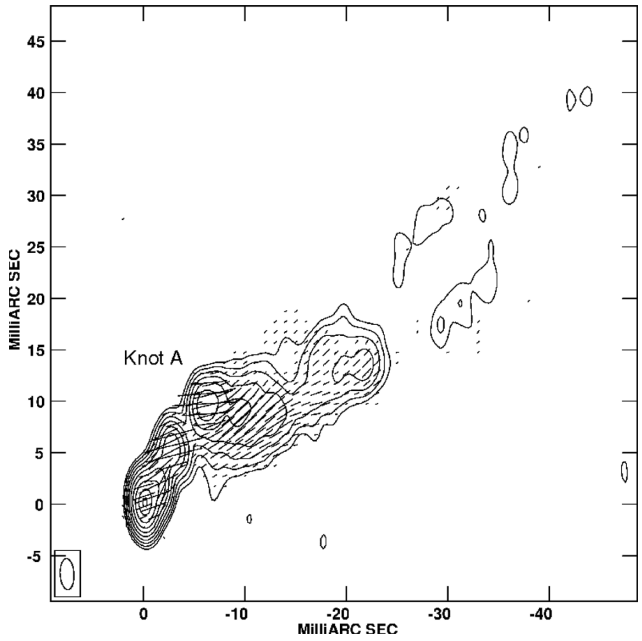



**Figure 1.** 4.99 GHz total intensity map of 3C 380 with magnetic field sticks superposed. The contours shown are −0.25, 0.25, 0.50, 1, 2, 4, 8, 16, 32, 64 and 95 per cent of the peak of 1.46 Jy beam$^{-1}$. The magnetic field sticks were obtained by rotating the calibrated polarization angles corrected for Galactic but not local Faraday rotation by 90°.

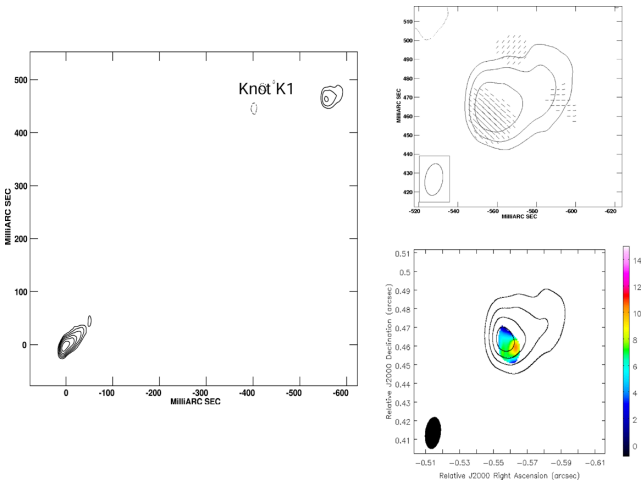



**Figure 2.** Left: 1.4 GHz total intensity map of 3C 380. The bottom contour is 1.7 per cent of the peak of 1.45 Jy beam$^{-1}$, and the contours increase in steps of a factor of 2. Top right: total intensity map of K1 with magnetic field sticks rotated such that they coincide with the fully Faraday-corrected values in the region where those are measured. Bottom right: two-frequency RM map of the region of K1 constructed using our 1.4 and 1.7 GHz polarization maps.

angles in the top-right figure have all been rotated by the amount required to make the polarization angles, at points where the two-frequency RM has been determined, agree with their fully Faraday-corrected values. Although we cannot guarantee that there is no residual Faraday rotation affecting the polarization angles in regions where the two-frequency RM values were not reliably measured, this seems unlikely, given the small local RM values and variations of these values over the region we have measured. Although the detected polarization is relatively weak, the overall morphology and magnetic field of the distant knot K1 at 1.4 GHz presented in Fig. 2 are similar to those reported by P2006 (see fig. 13 of that paper).

### 3.2 A transverse RM gradient: implications for the 3D magnetic field structure of the jet

Our new three-frequency RM measurements (Fig. 3) indicate that the assumption made by P2006 that the correct difference between their 1.6 and 5 GHz polarization angles was the smallest possible value was, in fact, incorrect: the $n\pi$ ambiguity is broken by the new three-frequency results presented here. Note that the integrated Faraday rotation measure reported by Rusk (1988) is +26 rad m$^{-2}$, so our observed RM values would have been slightly more positive if we had not removed the effect of the integrated (Galactic) RM from our polarization angle measurements.

The new RM map of the jet of 3C 380 within about 70 mas from the core displays relatively modest RM variations, but a transverse RM gradient is clearly visible roughly 10–30 mas from the core. This RM gradient spans roughly 3.5 beamwidths, and the difference in the RM values on opposite sides of the jet is roughly 4–5$\sigma$, making this a very firm detection.

Fig. 3 also shows RM values along a slice across the region of the RM gradient, which displays the monotonicity of the RM gradient, and demonstrates the significance of the RM differences, which is $\sim$4$\sigma$. Fig. 3 also shows plots of the EVPA $\chi$ versus the wavelength $\lambda$ squared for the four points along the slice shown. The adherence to linear $\lambda^2$ dependences is excellent. The RM uncertainties in Fig. 3 were determined using $\chi$ uncertainties estimated in individual pixels using the approach of Hovatta et al. (2012), without including the effect of uncertainty in the EVPA calibration, since this cannot introduce spurious RM gradients, as is discussed in Mahmud, Gabuzda & Bezrukovs (2009) and Hovatta et al. (2012). The ability of the 1.4 and 1.6 GHz measurements to resolve the $n\pi$ ambiguity in the observed polarization angles is immediately clear. This combined with the long 'lever arm' between the two lower frequencies and 5 GHz yields RM measurements in individual pixels with low uncertainties of no more than $\sim$2 rad m$^{-2}$ (these will increase somewhat if the EVPA calibration uncertainties are included in the $\chi$ errors).

There are two obvious, straightforward interpretations of the observed transverse RM gradient across the 3C 380 jet: an enhancement of the electron density along the northern edge of the jet, or the presence of a helical or toroidal magnetic field component associated with the jet. If the viewing angle of the jet in the jet rest frame is not too far from 90°, the RM gradient produced by a helical jet magnetic field will span both positive and negative RM values, providing a strong diagnostic for a helical-field origin for transverse RM gradients including RM values of both signs. However, the RM values shift to encompass only one sign as the viewing angle in the rest frame of the jet moves away from 90°, so that helical-field-induced transverse RM gradients need not encompass RM values of both signs. In the case of the 3C 380 jet, the observed RM values (after subtracting the effect of Faraday rotation in our Galaxy) are all positive (Fig. 3, upper left), so that the observed transverse RM gradient could, in principle, be due to a gradient in either the electron density or the line-of-sight magnetic field across the jet. However, if there were a higher electron density along the northern edge of the jet, we would expect the jet to be interacting with this material to some extent, likely enhancing the longitudinal magnetic field due to shear, and giving rise to an increase in the polarization

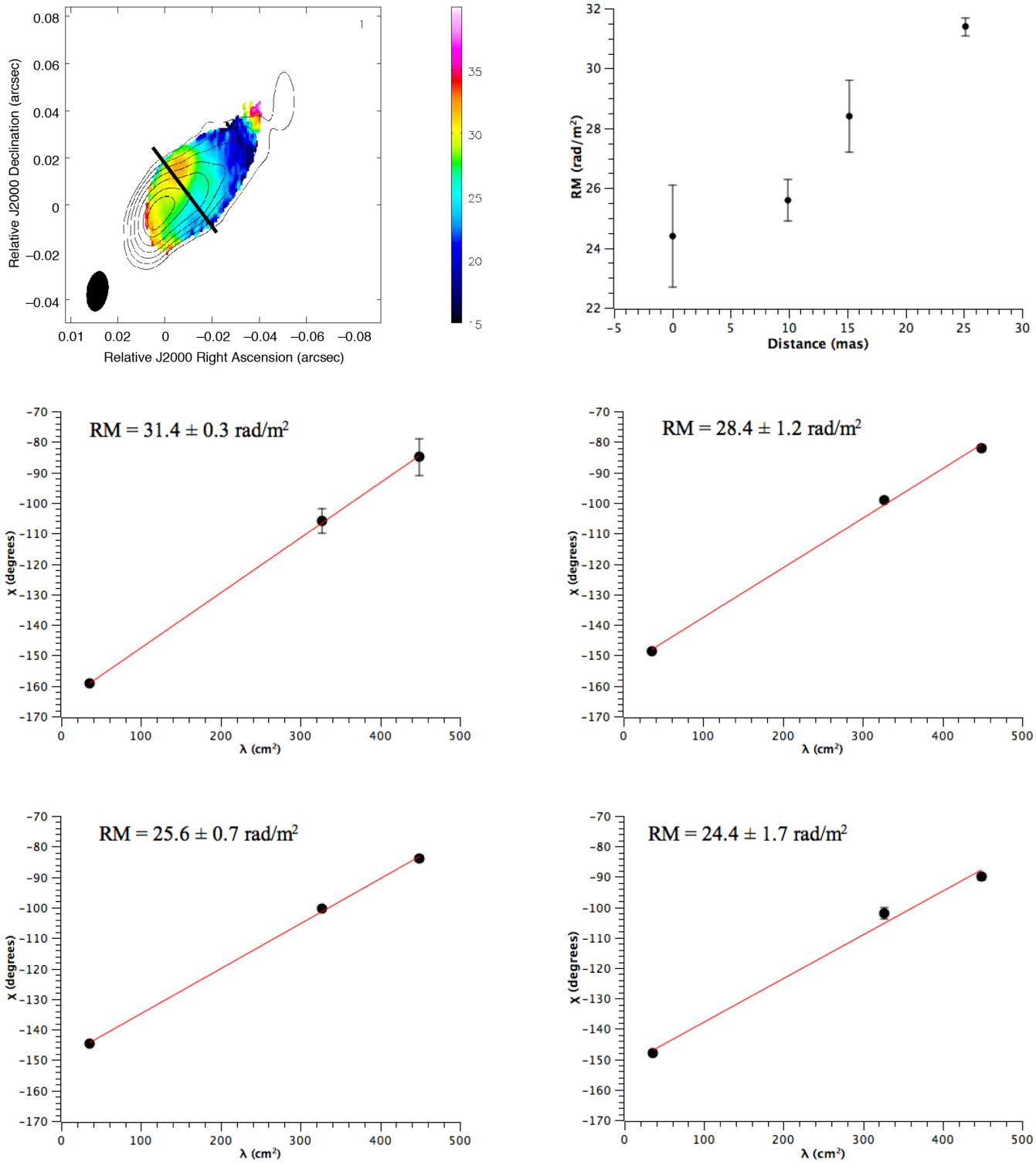



**Figure 3.** Upper left: 1.4 GHz total intensity map of the inner jet of 3C 380 with the distribution of the RM superposed. Upper right: RM values at four points along the slice across the jet shown by the bold line in the upper-left panel. The horizontal axis plots the distance along this slice starting from its Southwest end. Middle and lower rows: Plots of $\chi$ versus $\lambda^2$ for the four points shown in the slice above. The $\chi$ errors shown are $1\sigma$. The RM difference across this slice corresponds to about $4\sigma$.

along the northern edge of the jet, compared to the southern edge. In fact, Fig. 4 shows an increase in the degree of polarization along *both* edges of the jet, more consistent with the presence of a helical jet magnetic field than with a density enhancement along the northern side of the jet.

Earlier, shorter wavelength RM images of the inner 3C 380 jet by Taylor (1998) and P2006 showed no evidence for transverse RM structure across the jet. This is probably not surprising, since the RM uncertainties of those observations were considerably larger than the uncertainties of the observations considered here. The 1.4–1.6 GHz

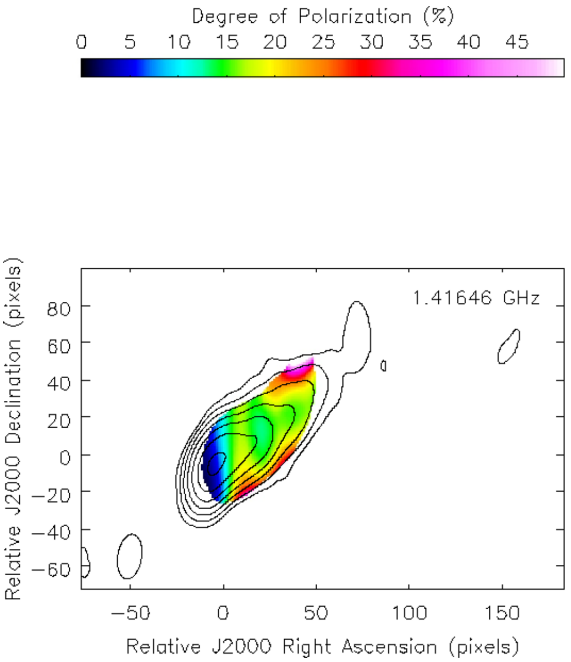



**Figure 4.** 1.4 GHz total intensity map of the inner part of the 3C 380 jet with the distribution of the degree of polarization superposed (in per cent).

RM map of the region of the knot K1, located roughly 0.7 arcsec from the core, likewise did not show evidence of systematic RM structure across the jet; in this case, this may suggest that the RM distribution has become dominated by a random component at this greater distance from the core.

## 4 CONCLUSION

This paper has presented new, total intensity polarization and Faraday RM measurements of the jet of 3C 380 based on simultaneous observations at 1.4, 1.7 and 5 GHz.

The results of the 1.4 and 1.7 GHz observations support the idea that the distant knot K1 investigated by P2006 is a conical shock in the jet flow in 3C 380. Higher sensitivity observations of this region are required to map out its total intensity and magnetic field structure in more detail.

Most interestingly, the three-frequency Faraday rotation measurements presented here have revealed a clear RM gradient across the jet at distances of about 10–30 mas from the core. The RM values spanned by this gradient correspond to differences of 4–5$\sigma$. This represents firm evidence that the jet of 3C 380 carries a helical or toroidal magnetic field component, which could naturally arise due to the rotation of the central black hole and its accretion disc. The importance of these new observations is that they suggest that this helical magnetic field component can survive to distances of hundreds of parsec from the central engine. At the same time, the 1.4–1.6 GHz RM map of the region of the knot K1, located roughly 0.7 arcsec from the core, did not show any evidence of systematic RM structure across the jet, suggesting that the RM distribution has become dominated by a random component at this greater distance from the core.

## ACKNOWLEDGEMENTS

The NRAO is a facility of the National Science Foundation operated under cooperative agreement by Associated Universities, Inc.

## REFERENCES

Asada K., Nakamura M., Inoue M., Kameno S., Nagai H., 2010, ApJ, 720, 41
Burn B. J., 1966, MNRAS, 133, 67
Cawthorne T. V., Wardle J. F. C., Roberts D. H., Gabuzda D. C., Brown L. F., 1993, ApJ, 416, 496
Croke S. M., O'Sullivan S. P., Gabuzda D. C., 2010, MNRAS, 402, 259
Gabuzda D. C., Mullan C. M., Cawthorne T. V., Wardle J. F. C., Roberts D. H., 1994, ApJ, 435, 140
Hallahan D. R., Gabuzda D. C., 2008, Proceedings of the 9th European VLBI Network Symposium on The Role of VLBI in the Golden Age for Radio Astronomy and EVN Users Meeting, p. 29, available at: http://pos.sissa.it/cgi-bin/reader/conf.cgi?confid=72
Healy F., Gabuzda D. C., 2013, Proc. 11th European VLBI Network Symposium, in press
Hovatta T., Lister M. L., Aller M. F., Aller H. D., Homan D. C., Kovalev Y. Y., Pushkarev A. B., Savolainen T., 2012, AJ, 144, 105
Kameno S., Inoue M., Fujisawa K., Shen Z.-Q., Wajima K., 2000, PASJ, 52, 1045
Lister M. L., Homan D. C., 2005, AJ, 130, 1389
Lister M. L. et al., 2009, AJ, 138, 1874
Lovelace R. V. E., Li H., Koldoba A. V., Ustyugova G. V., Romanova M. M., 2002, ApJ, 572, 445
Mahmud M., Gabuzda D. C., Bezrukovs V., 2009, MNRAS, 400, 2
Mahmud M., Coughlan C. P., Murphy E., Gabuzda D. C., Hallahan R., 2013, MNRAS, 431, 695
Nakamura M., Uchida Y., Hirose S., 2001, New Astron., 6, 61
O'Dea C. P., de Vries W., Biretta J. A., Baum S. A., 1999, ApJ, 117, 1143
Pacholczyk A. G., 1970, Radio astrophysics. Nonthermal Processes in Galactic and Extragalactic Sources. Freeeman & Co., San Franciso
Papageorgiou A., Cawthorne T. V., Stirling A, Gabuzda D, Polatidis A. G., 2006, MNRAS, 373, 449
Polatidis A. G., Wilkinson P. N., 1998, MNRAS, 294, 327
Rusk R. E., 1988, PhD thesis, Univ. Toronto
Taylor G. B., 1998, ApJ, 506, 637
Wilkinson P. N., Akujor C. E., Cornwell T. J., Saikia D. J., 1991, MNRAS, 248, 86

This paper has been typeset from a TEX/LATEX file prepared by the author.